

Graphene plasmonic nanogratings for biomolecular sensing in liquid

Meysam T. Chorsi^{1,2} · Hamid T. Chorsi³

Received: 12 June 2017 / Accepted: 3 November 2017 / Published online: 10 November 2017
© Springer-Verlag GmbH Germany, part of Springer Nature 2017

Abstract We design a surface plasmon resonance (SPR) molecular sensor based on graphene and biomolecule adsorption at graphene–liquid interfaces. The sensor configuration consists of two opposing arrays of graphene nanograting mounted on a substrate, with a liquid-phase sensing medium confined between them. We characterize the design in simulation on a variety of substrates by altering the refractive index of the sensing medium and varying the absorbance–transmittance characteristics. The influence of various parameters on the biosensor’s performance, including the Fermi level of graphene, the dielectric constant of the substrate, and the incident angle for plasmon excitation, is investigated. Numerical simulations demonstrate the sensitivity higher than 3000 nm/RIU (refractive index unit). The device supports a wide range of substrates in which graphene can be epitaxially grown. The proposed biosensor works independent of the incident angle and can be tuned to cover a broadband wavelength range.

1 Introduction

MID-infrared (MIR) and far-infrared (FIR) spectroscopy is a powerful characterization method for probing complex vibrational characteristics of biomolecules. The molecular

fingerprint of many molecules in bulk materials lies in the range of $350\text{--}4000\text{ cm}^{-1}$, ($\sim 2.5\text{--}30\text{ }\mu\text{m}$) which can be exploited to uniquely identify the fundamental molecular biomarkers of life, such as DNA, proteins, and lipids [1]. However, due to mismatch between spectral range in MIR ($\sim 10\text{ }\mu\text{m}$) and biomolecular dimensions ($\sim 10\text{ nm}$), the light–molecule interaction becomes remarkably feeble [2]. To circumvent this drawback, optical energy confinement in the near-field region of the surface can be used to increase the light–molecule interaction cross section. However, the diffraction limit affects an extremely weak field confinement. Surface plasmons (SPs) can be exploited to confine the optical energy of light in dimensions far beyond the diffraction limit. SPs are collective oscillations of conduction electrons excited via polarized light at the interface between a negative and positive permittivity material [3]. SPs were widely recognized in biosensing following the pioneering work of Liedberg and his colleagues in 1983 [4]. In their experiment, a He–Ne laser was used to excite SPs at the interface between a silver film and Human IgG in water solution. Then, the solution of anti-IgG was injected which resulted in a 0.3° shift of the resonance angle. Since then, biosensing based on SPs has made speedy progress. In 2006, Homola group reported a surface plasmon biosensor based on a special metallic grating with a profile composed of multiple harmonics [5]. The reflected light in this configuration contained multiple resonance peaks, one for each diffractive grating. The use of multiple resonance dips gave more detailed information about the refractive index distribution at the sensor surface. This approach significantly advances the conventional surface plasmon spectroscopy as it enables in situ measurements of general refractive index profiles. In 2011, Knoll group used localized SPs (LSPs)-enhanced fluorescence spectroscopy for the detection of *Escherichia*

✉ Meysam T. Chorsi
meysam.chorsi@uconn.edu

¹ Department of Mechanical Engineering, University of Connecticut, Storrs, CT 06269, USA

² Department of Biomedical Engineering, University of Connecticut, Storrs, CT 06269, USA

³ Thayer School of Engineering, Dartmouth College, Hanover, NH 03755, USA

coli (*E. coli* O157:H7). The limit of detection below 10 cfu mL⁻¹ was reported [6].

Noble metals such as silver and gold have traditionally been the materials of choice for plasmonic sensing due to their high electrical conductivities and large plasma frequencies at optical frequencies. Although silver has preferred optical properties to gold, it has been rarely used for bio-sensing applications due to its high oxidation susceptibility. On the other hand, gold, the popular choice, presents high losses at infrared frequencies due to intraband transitions which limit the confinement of SPs and reduce the sensitivity. Moreover, gold does not adsorb biomolecules ideally due to its intrinsic hydrophobicity and high chemical inertness.

Graphene, a single atomic plane of carbon atoms, has recently emerged as a revolutionary material due to its astounding physical properties, not least of which are its optical characteristics. It has been shown both theoretically and experimentally that graphene itself supports the propagation of surface plasmon waves in MIR and FIR regions with tunable Fermi energy levels [7]. Graphene plasmons have lower loss than Noble metal plasmons and display very strong lateral confinement due to shorter excitation wavelength of plasmon oscillations. Furthermore, graphene plasmon resonances can be tuned owing to their relativistic-like linear energy dispersion (Dirac cone). Charge carriers can be induced through chemical doping or electrostatic gating in the terahertz and infrared region. Compared to metal plasmons, plasmons on graphene are more strongly confined. In addition, due to π -stacking interactions (π -binding) and high surface-to-volume ratio, biomolecules adsorb strongly to the surface of graphene. These characteristics make graphene a suitable choice to be used for biosensing applications [8].

In this study, we have designed a label-free biomolecular sensing device with ultra-high sensitivity that operates at infrared frequency band. The device can achieve a sensitivity of over 3000 nm/RIU (refractive index unit), three times higher than that of current topnotch metal-based plasmonic biosensors.

2 Analysis and simulation results

The proposed structure of the graphene plasmonic biomolecular sensor is schematically illustrated in Fig. 1. The structure consists of two opposing arrays of graphene nanograting sitting on transparent substrates; The analyte-containing fluidic layer is placed between the substrates and is in direct interaction with the graphene nanograting arrays. The structure is illuminated via transverse magnetic (TM) polarized light from the top. The period and the nanograting width are 400 and 600 nm, respectively. The proposed structure can be realized using chemical vapor deposition

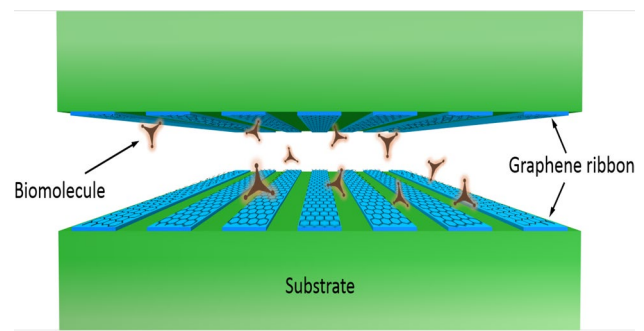


Fig. 1 Schematic of the graphene plasmonic biosensor. Arrays of graphene nanoribbons are periodically patterned onto the lower and upper transparent substrates; and the sensing medium, containing the liquid-phase biological molecules of interest, is sandwiched between them. The height of the channel is 1.1 μm

(CVD)-grown monolayer graphene and electron beam lithography to pattern the graphene into nanoribbons [1].

The electronic properties of graphene film have been intensely studied in the past 10 years [9]. In this work, graphene is modeled as a thin layer with a thickness of 0.34 nm, as the graphene layers are separated by ~ 0.34 nm in graphite. The conductivity of profile is calculated based on the Kubo formula [10]:

$$\begin{aligned} \sigma_{\text{graphene}}(\omega) &= \sigma_{\text{intra}}(\omega) + \sigma_{\text{inter}}(\omega) \\ &= \frac{2ie^2T}{\pi\hbar(\omega + i\tau^{-1})} \ln \left[2 \cosh \left(\frac{\mu_c}{2T} \right) \right] \\ &\quad + \frac{e^2}{4\hbar} \left[\theta(\omega - 2\mu_c) - \frac{i}{2\pi} \ln \frac{(\omega + 2\mu_c)^2}{(\omega - \mu_c)^2} \right], \end{aligned} \quad (1)$$

where, e is the electron charge, \hbar is the reduced Planck's constant, ω is the radian frequency, $\theta(\omega - 2\mu_c)$ denotes a step function, μ_c is the chemical potential (Fermi energy level), τ is the momentum relaxation time, and T is the temperature. The chemical potential depends on the carrier density and can be controlled by electrostatic or chemical doping. In this work, the following parameters were used: $t = \mu E_F / ev_F^2 = 0.1$ ps, moderate carrier mobility $\mu \approx 10^3$ cm²/(V·s), Fermi velocity $v_F \approx 10^6$ m/s, $T = 300$ K, and the chemical potential $\mu_c = 0.7$ eV. The first term in Eq. 1 (Drude-like form) describes the intraband carrier relaxation contribution, and the second term describes the interband carrier transition contribution. As it can be seen from Eq. 1, the propagation of SPPs on graphene is largely dependent on the Fermi level. The resonance wavelength at transmission (λ_R) for graphene nanograting with width d can be expressed as follows [11]:

$$\lambda_R = 2\eta d \text{Re} \left(\frac{k_p}{k_0} \right), \quad (2)$$

in which k_0 is the free space wavevector and

$$\eta = \frac{2e^2 E_F}{\omega(\omega + i\tau^{-1})\hbar^2 \zeta d}, \quad k_p = \frac{ic(\epsilon_{mf} + \epsilon_s)\epsilon_0}{\sigma_{\text{graphene}}(\omega)} k_0, \quad (3)$$

where ζ is the dielectric constant of material around graphene, and ϵ_s and ϵ_{mf} are the relative permittivity of substrate and fluidic layer, respectively. Plugging Eq. (3) into Eq. (2), and considering the infrared conductivity for intra-band transitions:

$$\lambda_R = \frac{2\pi c \hbar}{e} \sqrt{\frac{\eta(\epsilon_{mf} + \epsilon_s)d}{E_F}}. \quad (4)$$

Equation (4) shows that the transmission resonance of graphene grating shifts via change in the refractive index of the fluidic sensing medium. The performance of the proposed plasmonic biosensor is evaluated based on sensitivity. The sensitivity is defined as the ratio of the shift in resonance wavelength ($\Delta\lambda_p$) to the refractive index (RI) change in the sensing medium and is calculated via the following formula [12]:

$$SE = \frac{\Delta\lambda_R}{\Delta n_s} = \frac{2\pi c \hbar \eta n_s}{e \sqrt{n_s^2 + \epsilon}} \sqrt{\frac{(\epsilon_0)d}{E_F}}. \quad (5)$$

The simulations in this letter were performed using the finite-element method (FEM) which is a widely accepted method for modeling electromagnetic and wave propagation problems (implemented in COMSOL Multiphysics).

The characteristics of monolayer graphene nanograting become more distinct by comparing its near-field confinement to that of a state-of-the-art metallic plasmonic sensors composed of gold. Figure 2 presents the computed percentage of near-field intensity confinement within a given distance f from the structure for a gold and graphene nanograting. From Fig. 2, it can be observed that more than 90% of near-field energy is confined within 20 nm from the graphene surface, while for the gold, most of the energy is spread over a distance of about 400 nm away from the gold surface. This shows the strong near-field energy restriction in graphene and tighter plasmon confinement. Next, we study the graphene plasmonic confinement at the liquid-graphene interface.

Figure 3 presents the effect of the Fermi level on the electric field and stored energy for a graphene nanoribbon in contact with a fluidic (H_2O) layer. Graphene nanoribbon is placed at the interface of the fluidic layer and silica substrate.

From Fig. 3a, it can be clearly seen that increasing the Fermi level increases the electric field intensity distribution on top of graphene. On the other hand, the near-field energy confinement gets stronger on the graphene ribbon as Fermi level increases, as it can be seen in Fig. 3b. The higher near-field confinement provides higher RI sensitivity for biomolecule adsorption.

To select a proper substrate for the biosensor, commonly used materials such as MgF_2 , poly (methyl methacrylate) (PMMA), SiO_2 , SiC, and Si were chosen. The refractive index range of the sensing media has been varied from $n = 1.3$ to $n = 1.53$ to underline the sensitivity of the device. Here, we examine a lossless scenario by only considering the real part of the refractive index to characterize the sensitivity

Fig. 2 Near-field intensity confinement. More than 90% of near-field energy are confined within 20 nm from the graphene surface (at wavelength $\lambda = 17 \mu\text{m}$)

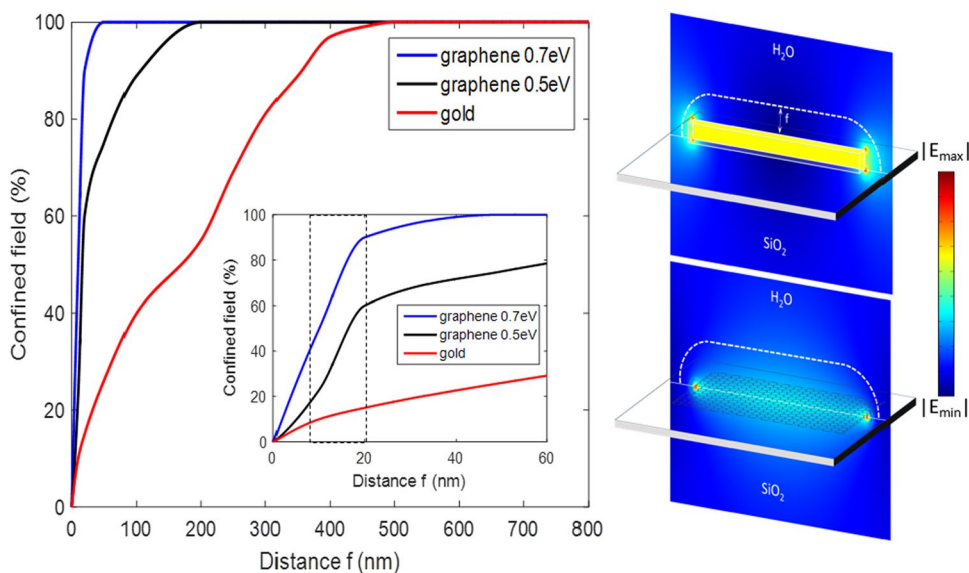
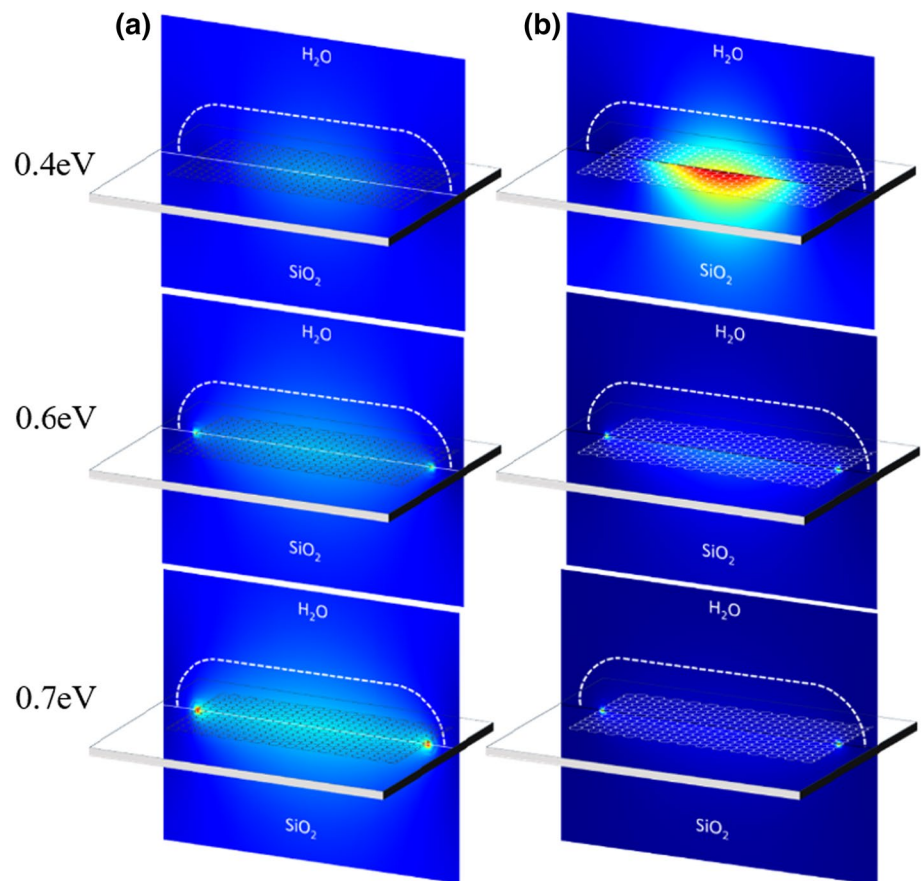


Fig. 3 Plasmonic properties of single-layer graphene in liquid for different Fermi level values (0.4, 0.6, and 0.7 eV). **a** Electric field intensity, $|E|$, **b** stored power (W/m^2)



of the proposed structure. For more realistic scenarios, the imaginary part of the refractive index (optical loss) needs to be considered. To select a proper substrate, the transmission spectrum was simulated for substrates with various dielectric constants in Fig. 4a, b. It can be seen that the transmission spectrum shows a red-shift with increasing the substrate permittivity. Moreover, the quality factor of the transmission resonances decreases and the transmission width gets wider. The sensitivity for the test substrates is summarized in Fig. 4c.

The highest sensitivity is 3053 nm/RIU for the lowest RI substrate, MgF_2 . This value is three times higher than the sensitivity of current superior gold-based plasmonic biosensors [13]. The high sensitivity of graphene can be explained owing to the short wavelength of graphene plasmons, which decreases the group velocity and increases the interaction time between biomolecules and light. Using two layers of graphene implements two levels of molecule-plasmon interaction and enables larger plasmonic resonance shift. The electric field distribution on top of the graphene nanogratings, when they are illuminated from the top with a transverse magnetic polarization at normal incidence, is shown in Fig. 4d. The effect of graphene structure on the sensitivity of

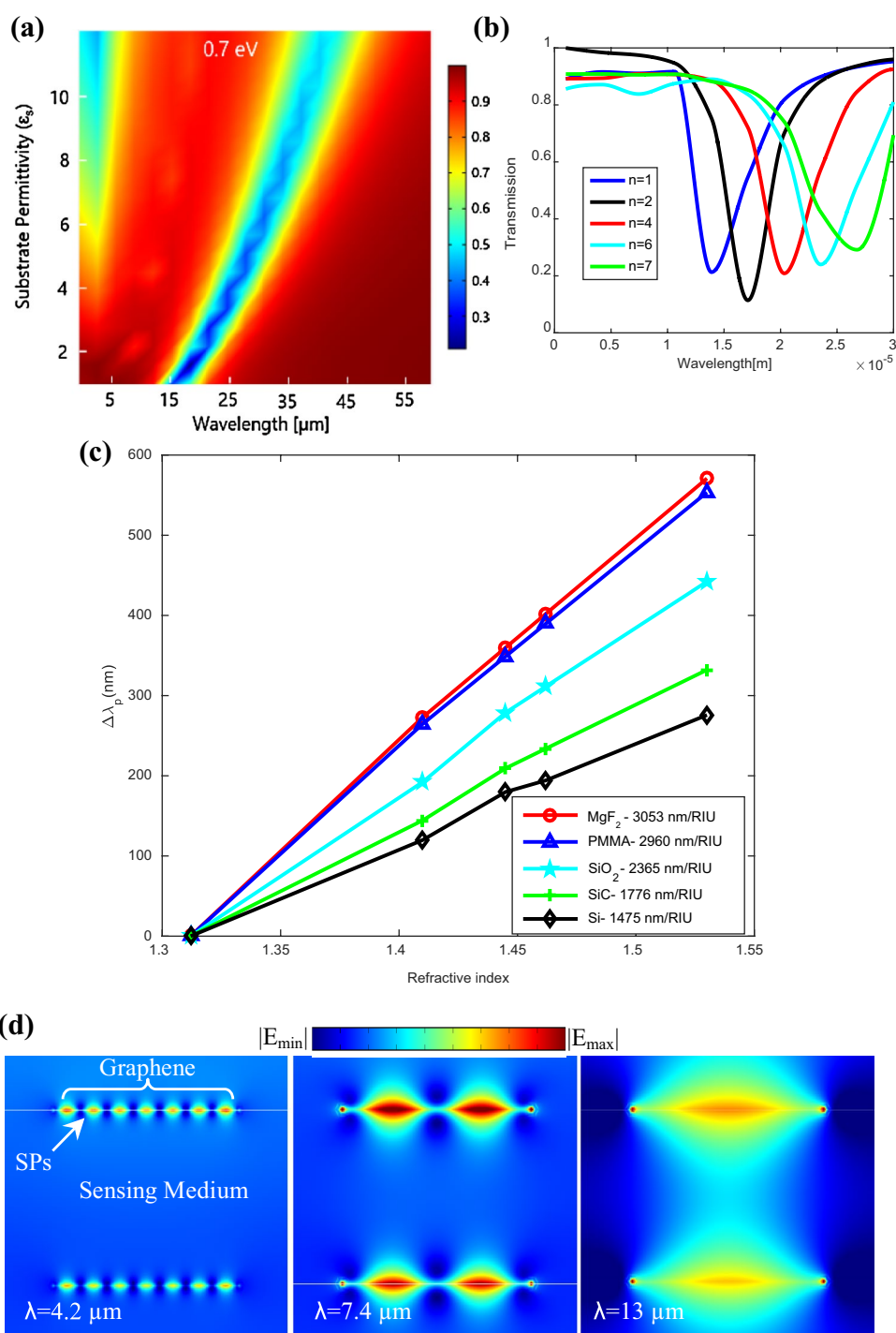
the biosensor is also studied and the results are presented in Fig. 5. Figure 5a shows the transmission spectrum as a function of graphene nanograting width (d) with period (p) fixed at 400 nm. It can be observed that the resonance wavelength has redshifted to longer wavelengths with increasing width, in agreement with Eq. (4). Furthermore, the resonance dip broadens for larger graphene width which is mainly due to field confinement decrease.

Finally, we have analyzed the effect of Fermi level on the performance of the plasmonic biosensor. The results are depicted in Fig. 6. It can be seen that the resonance minimum shows blue shift with increasing the Fermi level. The dashed line shows that resonance peak has shifted from 24.5 μm for 0.4 eV to 18.9 μm for $\epsilon_{mf} = 1.3$. The plasmonic resonance width gets narrower with increasing the Fermi level, which is consistent with Eq. (4).

3 Conclusion

In summary, we design an ultrasensitive biomolecular sensing device in which plasmon oscillations on graphene

Fig. 4 Effect of the substrate. **a, b** Transmission spectrum for $\epsilon_{mf} = 1.3$ and $1 \leq \epsilon_s \leq 12$. **c** Sensitivity for five frequently used substrates with different dielectric constants. The sensing medium changes from $n = 1.3$ to $n = 1.53$. Inset shows sensitivity per refractive index change. **d** Electric field distribution, $|E|$ on top of a graphene nanoribbon. Here, $\epsilon_{mf} = 1.3$, $\epsilon_s = 2$, and λ is the wavelength



are utilized to detect changes in the refractive index of the analyte. The novel double layer nanograting structure enables high molecule–graphene plasmon interaction which enhances the sensitivity. Numerical simulations demonstrated a sensitivity as high as 3053 nm/RIU. The effect of different parameters including the substrate permittivity, design structure, and the electrical properties of graphene

has been studied in detail to optimize the sensitivity. It has been shown that the dynamic tunability of graphene can enable the detectable refractive index changes covering a broad wavelength range from infrared to THz. The combined high sensitivity and specificity of our biomolecular sensors holds promise for potential breakthroughs in lab-on-chip-type clinical diagnostics at point-of-care to facilitate precision healthcare.

Fig. 5 Effect of the graphene width and period for $E_f = 0.7$ eV and MgF_2 substrate. **a** Transmission spectrum with varying nanograting width d , **b** sensitivity for periods of 200, 300, 400, and 500 nm, respectively; the sensing medium changes from $n = 1.3$ to $n = 1.53$

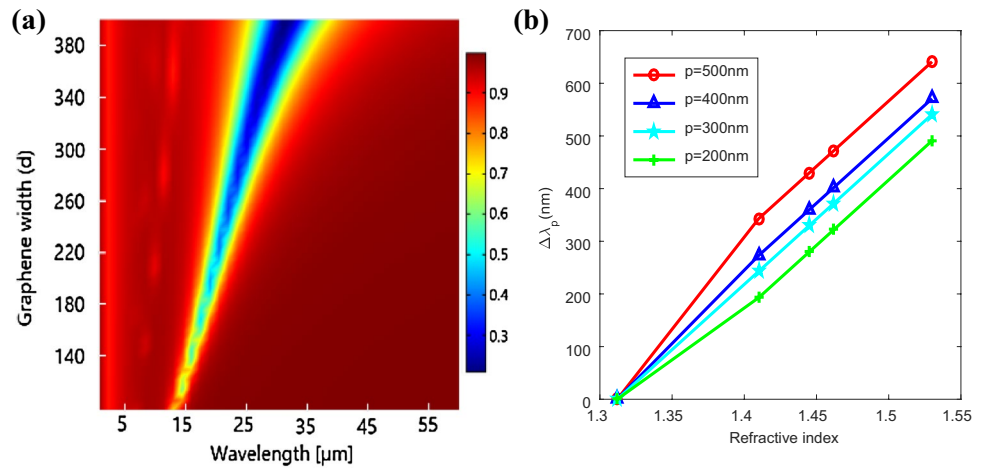
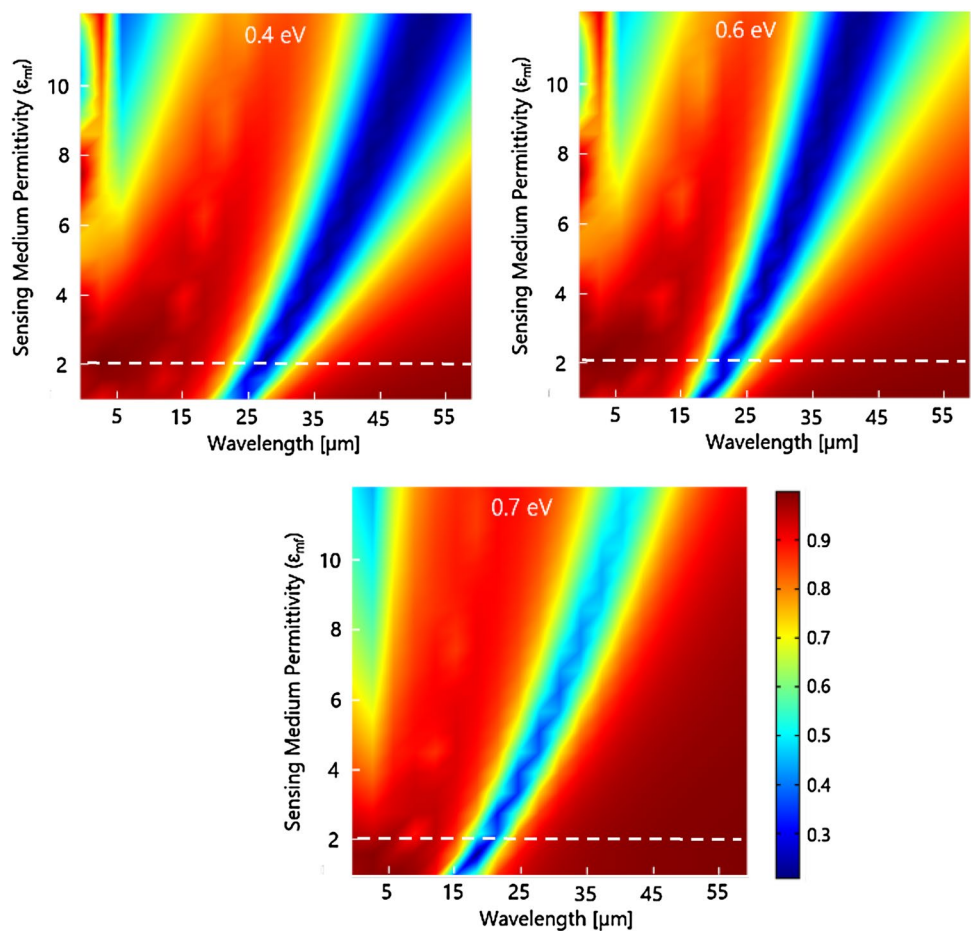


Fig. 6 Effect of the substrate permittivity. Sensing medium permittivity has changed from 1 to 12 and the permittivity of the liquid layer is kept constant at 1.3



Acknowledgements The authors thank Prof. John X.J. Zhang from Dartmouth College and Prof. Stephen D. Gedney from the University of Colorado Denver for the fruitful discussion and guidance.

References

1. D. Rodrigo, O. Limaj, D. Janner, D. Etezadi, F.J. García de Abajo, V. Pruneri et al., Mid-infrared plasmonic biosensing with graphene. *Science* **349**(6244), 165–168 (2015)
2. H. Hu, X. Yang, F. Zhai, D. Hu, R. Liu, K. Liu et al., Far-field nanoscale infrared spectroscopy of vibrational fingerprints of

- molecules with graphene plasmons. *Nat. Commun.* **7**, 12334 (2016)
3. H.T. Chorsi, S.D. Gedney, Efficient high-order analysis of bow-tie nanoantennas using the locally corrected Nystrom method. *Opt. Express* **23**(24), 31452–31459 (2015)
 4. B. Liedberg, C. Nylander, I. Lunström, Surface plasmon resonance for gas detection and biosensing. *Sens. Actuators* **4**, 299–304 (1983)
 5. P. Adam, J. Dostálek, J. Homola, Multiple surface plasmon spectroscopy for study of biomolecular systems. *Sens. Actuators B* **113**(2), 774–781 (2006)
 6. C.-J. Huang, J. Dostalek, A. Sessitsch, W. Knoll, Long-range surface plasmon-enhanced fluorescence spectroscopy biosensor for ultrasensitive detection of *E. coli* O157:H7. *Anal. Chem.* **83**(3), 674–677 (2011)
 7. A.N. Grigorenko, M. Polini, K.S. Novoselov, Graphene plasmonics. *Nat. Photon* **6**(11), 749–758 (2012)
 8. H.T. Chorsi, M.T. Chorsi, X.J. Zhang, Using graphene plasmonics to boost biosensor sensitivity. *SPIE Biomed. Opt. Med. Imag.* (2016). <https://doi.org/10.1117/2.1201610.006712>
 9. D. Wei, Y. Liu, Y. Wang, H. Zhang, L. Huang, G. Yu, Synthesis of N-doped graphene by chemical vapor deposition and its electrical properties. *Nano Lett.* **9**(5), 1752–1758 (2009)
 10. V.P. Gusynin, S.G. Sharapov, J.P. Carbotte, Magneto-optical conductivity in graphene. *J. Phys. Condens. Matter* **19**(2), 026222 (2007)
 11. T. Holmgaard, S.I. Bozhevolnyi, Theoretical analysis of dielectric-loaded surface plasmon-polariton waveguides. *Phys. Rev. B* **75**(24), 245405 (2007)
 12. J. Hu, X. Sun, A. Agarwal, L.C. Kimerling, Design guidelines for optical resonator biochemical sensors. *J. Opt. Soc. Am. B* **26**(5), 1032–1041 (2009)
 13. J. Homola, S.S. Yee, G. Gauglitz, Surface plasmon resonance sensors. *Sens. Actuators B* **54**(1), 3–15 (1999)